Research on Chemical Intermediates Volume 46, April 2020, pp. 2403–2416
DOI: 10.1007/s11164-020-04098-8

Methylation of 2-methylnaphthalene over metal impregnated mesoporous MCM-41 for the synthesis of 2,6-triad dimethylnaphthalene isomers

Aysel Niftaliyeva[1*], Fatih Güleç[2,3], Ali Karaduman[4]

[1] Chemical Engineering, Faculty of Engineering, Selçuk University, Konya, 42030, Turkey
[2] Chemical Engineering, Faculty of Engineering, University of Nottingham, Nottingham, NG7 2RD, UK
[3] Energy and Power Theme, School of Water, Energy and Environment, Cranfield University, Cranfield, MK43 0AL, UK
[4] Chemical Engineering, Faculty of Engineering, Ankara University, Ankara 06100, Turkey

*Aysel.Niftaliyeva@gmail.com

Abstract

2,6-dimethyl naphthalene (2,6-DMN) is one of the key intermediates for the production of polyethylene naphthalate (PEN), which demonstrates superior properties compared with the Polyethylene terephthalate (PET). However, the complex synthesis procedure of 2,6-DMN increases the production cost and decrease the comorcelisation of PEN. In this study, selective synthesis of 2,6-triad DMN isomers (1,5-DMN, 1,6-DMN and 2,6-DMN) have been investigated by the methylation of 2-methylnaphthalene (2-MN) over mesoporous Cu/MCM-41 and Zr/MCM-41 zeolite catalysts. On the contrary of other DMN isomers, 2.6- triad isomers can effectively be converted to be profitable 2,6-DMN with an additional isomerisation reaction, which is a new approach to reach higher 2,6-DMN yield. The methylation reactions of 2-MN were investigated in a fixed-bed reactor at 400 °C and weight hourly space velocity (WHSV) of 1-3 h^{-1}. The results showed that the activity of MCM-41 on the methylation of 2-MN has been enhanced with the impregnation of Cu. The conversion increased from about 17 % to 35 wt. % with the impregnation of Cu. Similarly, the 2,6-triad DMN selectivity and 2,6-/2,7-DMN ratio reached the maximum level (48 wt. % and 1.95, respectively) over Cu impregnated MCM-41 zeolite catalyst.

Keywords: Methylation, 2-methylnaphthalene, 2,6-dimethylnaphthalene, 2,6-triad DMN, MCM-41, PEN.

1. Introduction

2,6-dimethylnaphthalene (2,6-DMN) is one of the most convenient chemicals using in the synthesis of 2,6-naphthalene-dicarboxylic acid, which is the monomer being used to production of polyethylene naphthalate (PEN). Superior properties of PEN such as thermal, mechanical and chemical stability, high gas barrier, high tensile strength, heat resistance, high stability against UV and X-ray, enable to be a better polymer in industrial applications compare to PET [1-6]. However, the commercialisation of PEN has been limited due to the excessive production cost of 2,6-DMN. Therefore, the studies have been recently focused on an alternative method for the selective synthesis of 2,6-DMN by alkylation (methylation) of naphthalenes /methylnaphthalenes [7], disproportionation of methylnaphthalenes [8, 9] and isomerisation of dimethylnaphthalenes [10]. Thanks to these synthesis processes, ten different DMN isomers can be obtained, which consists of 2,6-triad (1,5-DMN; 1,6-DMN; 2,6-DMN), 2,7-triad (1,8-DMN; 1,7-DMN; 2,7-DMN), 2,3-triad (1,4-DMN; 1,3-DMN; 2,3-DMN) and 1,2-DMN [5, 10-12].

Studies on DMN synthesis mainly focus on heterogeneous shape-selective zeolites catalysts because of their controllable porous structures and surface acidic characteristics, strong thermal and water stability, large surface area and broad pore [13]. The methylation of naphthalene was investigated over HZSM-5, Hβ, HUSY and SAPO-11 zeolites modified by 0.1wt% PdO under atmospheric pressure. The stability of reaction, the highest 2,6-DMN selectivity, 2,6-DMN/2,7-DMN ratio and long catalyst lifetime were enhanced after modified by PdO_2 [2]. NH_4F and Pt modified HZSM-5 zeolites can be used for 2-MN methylation with methanol. The catalytic activity and products distribution depend strongly on zeolite acidity. The conversion of 2-MN and selectivity of 2,6-DMN change with the addition of Pt and the increase in the content of NH_4F [5]. Güleç et al. [14] also investigated Fe modified ZSM-5 zeolite on the methylation of 2-MN. The selectivity of 2,6-DMN in the methylation of 2-MN increased while the conversion decreased by the steam and TEOS modification of HZSM-5 zeolite [15]. Under high-pressure reaction conditions, compared with macro-sized MTW type zeolites, nano-sized MTW-type zeolites exhibited higher 2-MN conversion and dimethylnaphthalene (DMN) selectivity[16]. Niftaliyeva et al. [17] studied methylation of 2-MN over La and Cu modified Y zeolite. The results show that Cu modified catalysts show higher 2-MN conversion compared with parent Y zeolite. Recently, various medium and large-pore zeolite catalysts, mainly ZSM-5, ZSM-11, ZSM-12, MCM-22, Mordenite, beta, Y zeolite have been utilised as catalysts in the methylation of 2-MN and naphthalene [5, 17-21].

However, without a selective catalyst, in addition to 2,6-DMN, the other DMN isomers are also produced by methylation of naphthalenes. The similarity of the chemical and physical properties of DMN isomers complicates the separation of these substances [22]. Wang et al. [23] and Fang et al. [24] reported that the reactivity of the C-6 position is higher than the C-7 position since the electron density at C-6 is remarkably higher than that at C-7 on the methylation of 2-MN inside of catalyst channel. Therefore, 1,5-DMN and 1,6-DMN in the 2,6-triad group are also considered as valuable products which can be easily isomerised to 2,6-DMN [25-27]. It is reasonable to evaluate the overall selectivity for 2,6- triad DMN with the sum of 2,6-, 1,6- and 1,5-DMNs synthesised from the methylation of 2-MN as mentioned by Zhang et al. [2] and Güleç et al. [8].

MCM-41 zeolite has attracted considerable catalytic performance for selective methylation due to its periodic framework of regular mesopores, large surface area (> 1000m^2/g), high porosity (50-500 Å), highly uniform hexagonal structure of tuneable size, which helps the mass transfer of relatively large molecules of reactants to active sites in pores, excellent thermal stability (1173 K) [28-34]. The combination of large pores and mild acidity in Al-containing MCM-41 has enabled to use in a wide range of application such as alkylation, cracking and hydrocracking [29, 34-38]. Although pure MCM-41 has very weak acidity, it exhibits low acidity in the presence of Al in small quantities, in consequence of Al-atoms does not exist in the structure of MCM-41 compared to other zeolites. The addition of Al-atoms into the MCM-41 structure can produce active sites with Bronsted acid sites for adsorption, ion exchange and catalysis. For instance, García-Sancho et al. [39], Ding et al. [40], Güleç et al. [41], Juarez et al. [42] have investigated Zr- and/or Cu- modified MCM-41 samples on different reactions. They found that the acidity of MCM-41 can be enhanced by adding metals such as Zr and Cu.

However, the catalytic performance of Cu- and/or Zr- modified MCM-41 zeolite catalysts have not been investigated for the methylation of 2-MN, which is the novelty of the present work. Therefore, in this study, the methylation of 2-MN has been investigated in a fixed-bed reactor over MCM-41 and Cu-, Zr- impregnated MCM-41 zeolite catalysts. The conversion of 2-MN, the ratio of 2,6-DMN/2,7-DMN and the selectivity of 2,6-triad DMN are investigated to demonstrate the catalytic performance of the MCM-41 type zeolite catalysts.

2. Experimental

2.1 Impregnation of Cu- and Zr- on mesoporous MCM-41

Mesoporous MCM-41 (surface area 900 m^2/g) zeolite was obtained from Zeolyst (USA) in the form of powder. Before the impregnation of Cu- and Zr- metals, MCM-41 were mechanically mixed with γ-Al_2O_3 with a ratio of 5:1 and then cylindrical pellets were prepared from the mixture of MCM-41/γ-Al_2O_3 (after this point, the MCM-41 represents a mixture of MCM-41/γ-Al_2O_3 having a ratio of 5:1). The pellets were then dried at 393 K for 4 h and calcined 823 K for 6 h, respectively. The calcined pellets were used for the preparation of metal, Cu- and Zr- and bimetal, Cu/Zr, modified mesoporous MCM-41 zeolite catalysts. The wet impregnation method was carried out for the modification of mesoporous MCM-41 and the process was reported in our previous publications [8, 9, 14, 17, 41]. Briefly, for the preparation of Cu/MCM-41 (10 wt.% of Cu) and Zr/MCM-41 (10 wt.% of Zr), 3.31 gm of $Cu(NO_3)_2.3H_2O$ and 2.23 gm of $ZrO(NO_3)_2.xH_2O$ (ACROS, 99.5 %) were dissolved in 20 ml of deionized water respectively. Then, 8 gm of MCM-41 was added into the aqueous solutions. Cu/Zr/MCM-41 (5 wt.% of Cu-Zr) catalyst was also prepared using 1.60 gm of $Cu(NO_3)_2.3H_2O$ and 1.067 gm of $ZrO(NO_3)_2.xH_2O$. The impregnation was held at room temperature for 24 h. The mixture was then dried at 393 K for 4 h and calcined at 823 K for 6 h. After the calcination, parent MCM-41, Cu/MCM-41, Zr/MCM-41, and Cu/Zr/MCM-41 catalysts were prepared.

2.2. Characterization of the prepared catalysts

The pore structure of the catalysts was measured by Nitrogen adsorption-desorption isotherms at liquid nitrogen temperature (77 K) using the Quantachrome NOVA 2200 series volumetric gas adsorption instrument. In order to examine the surface area of the prepared catalysts were measured according to the BET (Brunauer–

Emmett–Teller) method using the nitrogen adsorption isotherm data and mesoporous size distributions of the samples were determined using the BJH (Barrett, Joyner and Halenda) method. The X-ray diffraction patterns of the catalysts were obtained using a Bruker D8 Advance with DaVinci X-ray diffractometer (XRD) with Cu-Kα radiation at 40 kV. The scanning range was set from 5° to 90° (2θ). Additionally, the IR spectroscopy of adsorbed pyridine (Py-IR) was carried out on a Mattson 1000 Fourier transform infrared spectrometer (FTIR) to identify the Brønsted and Lewis acid sites present in each material. About 1g of the sample was weighed and treated with pyridine before prepared pellets. After a background spectrum was recorded, the pyridine absorbed samples were scanned. The scanning electron microscopy (SEM) images and Elemental analysis of the samples were performed using an energy dispersive X-ray spectrometer (EDX) analysis were performed using a ZEISS EVO 40 microscope with an accelerating voltage of 20 kV. The samples were carbon-coated prior to the SEM investigation. The quantitative chemical analysis of chemical elements of prepared catalysts based on the measurements of the wavelengths and intensities of their X-ray spectral lines emitted by secondary (emissions) excitation were identified using a Spectra XLAB-2000 PEDX-ray fluorescence (XRF).

2.3. Catalytic activity of the prepared catalysts

The methylation of 2-methylnaphthalene (as demonstrated in Figure 1) was investigated over the prepared zeolite catalysts, MCM-41, Cu/MCM-41, Zr/MCM-41, and Cu/Zr/MCM-41, using a fixed-bed experimental set-up, which has already presented in our previous publications [8, 9, 14, 17, 41]. As demonstrated in our previous studies, a fixed-bed reactor having a length of 30 cm and diameter of 1 cm is located in a tubular furnace where the temperature is controlled by both a thermocouple connected by the catalyst bed and a PID temperature controller connected by furnace itself. The volumetric flow rate of the methylation feed consisting of 2-MN, methanol and 1,3,5-trimethyl benzene (mesitylene) having a molar ratio of 1:5:5 is adjusted using ISCO Model 2350 HPLC Pump.

Approximately 1.0 g of zeolite catalyst which was pelletised in the shape of a cylindrical was firstly placed in the middle zone of the reactor which was located in a high-temperature tubular furnace. Before the methylation tests, the catalysts were activated at 500 °C under a nitrogen flow of 5 mL/min for about 30 min to purify the pores from the water. After the catalyst activation, the temperature was then down to the reaction temperature. The methylation experiments were carried out at 400 °C and three different weight hourly space velocities, WHSV: 1 h^{-1}, 2 h^{-1}, 3 h^{-1}. The reaction products were condensed at -10 °C and separated from gases using a phase separator. The products were then analysed by gas chromatography (GC; Thermo Finnigan DSQ250) equipped with mass spectroscopy (MS; Zebra brand capillary column having a length of 60 m internal diameter of 0.25 mm and the film thickness of 0.25 µm working -60 to 370 °C). The conversion of 2-MN, the selectivity of 2,6-triad dimethylnaphthalene and the ratio of 2,6-DMN/2,7-DMN were determined using the following equations;

$$Conversion\ of\ 2-MN = \left[\frac{W_{2-MN,0} - W_{2-MN,t}}{W_{2-MN,0}}\right] * 100 \quad (1)$$

$$2{,}6-triad\ DMN\ seceltivity = \left[\frac{W_{2,6-triad\ DMN}}{W_{DMNs}}\right] * 100 \quad (2)$$

$$2{,}6-/2{,}7-DMN\ ratio = \left[\frac{W_{2,6-DMN}}{W_{2,7-DMN}}\right] \quad (3)$$

$W_{2\text{-MN},0}$, and $W_{2\text{-MN},t}$ are the weight of 2-MN in the feed and product mixtures, respectively. The 2,6-triad DMN selectivity is the mass percentage of 2,6-DMN, 1,6-DMN and 1,5-DMN in total DMN isomers. W_{DMNs}, $W_{2,6\text{-DMN}}$ and $W_{2,7\text{-DMN}}$ are pointing the weight percentage of total DMN isomers, 2,6-DMN, 2,7-DMN, respectively.

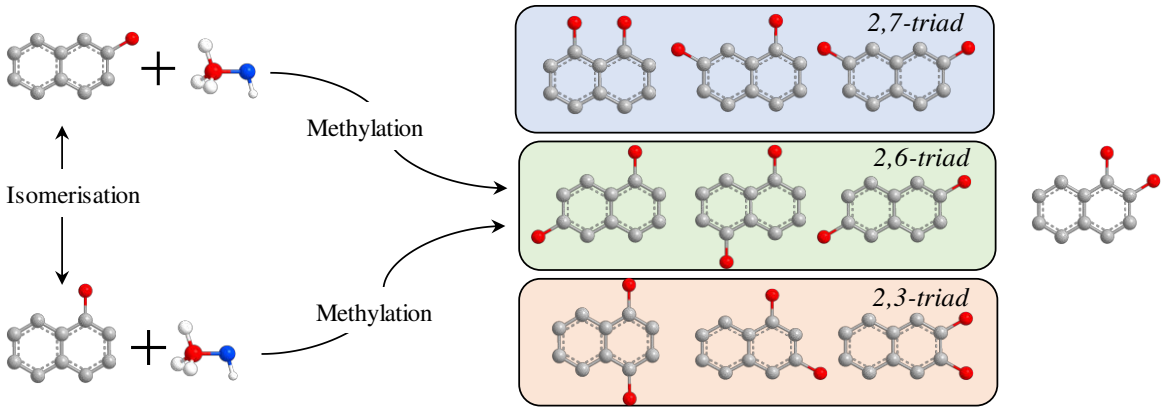

Figure 1. Possible reaction pathways for the methylation of 2-MN.

3. Results and Discussion

3.1. Characterization of prepared catalysts

The N_2 adsorption-desorption isotherms and mesopore size distributions of the prepared catalysts are demonstrated in Figure 2 and Table 1. Figure 2 shows that the isotherms of the prepared MCM-41 samples demonstrate adsorption of monolayer-multilayer and capillary condensation trends on the outer particle surfaces, which named hysteresis with a sharp inflexion value of P/P_0 is higher than 0.4. Apparently, MCM-41 samples show capillary condensation step, is indicating a uniformity of the mesopore size distribution having a diameter of 2–50 nm with type IV isotherm according to International Union of Pure and Applied Chemistry (IUPAC) classification [34, 40, 42]. The capillary condensation step of metal impregnated MCM-41 samples start earlier than parent MCM-41 due to a contraction in pore diameter (as seen in Table 1) [43].

Table 1. BET surface area, BJH Pore volume and pore diameter of the prepared catalysts.

Catalyst*	Surface area, (BET) (m^2/g)	Pore volume, (BJH) (cm^3/g)	Pore diameter, (BJH) (Å)
MCM-41	833.1	0.717	37.21
Cu/MCM-41	742.2	0.808	31.03
Zr/MCM-41	773.9	0.683	30.94
Cu/Zr/MCM-41	631.0	0.678	30.98

* MCM-41 represents the mixture of MCM-41/γ-Al_2O_3 having a ratio of 5:1.

Table 1 demonstrates that the BET surface area decreased from 833 m^2/g to about 742, 773, and 631 m^2/g with the impregnation of Cu, Zr, and Cu/Zr, respectively. Similarly, the BJH pore diameter has also demonstrated a decrease with the impregnation of metal and bimetal into MCM-41 zeolite pores. However, pore volume demonstrates an increase from about 0.72 cm^3/g to 0.81 cm^3/g with the impregnation of Cu, although it has insignificantly affected by the impregnation of Zr and Cu/Zr. The decrease in the surface area by the impregnation of metals maybe therefore attributed to pore blocking by the impregnation. As the micropores in

the zeolite frames tend to block by the impregnation of metals, which makes disable these surfaces in the micropores [8, 44-46].

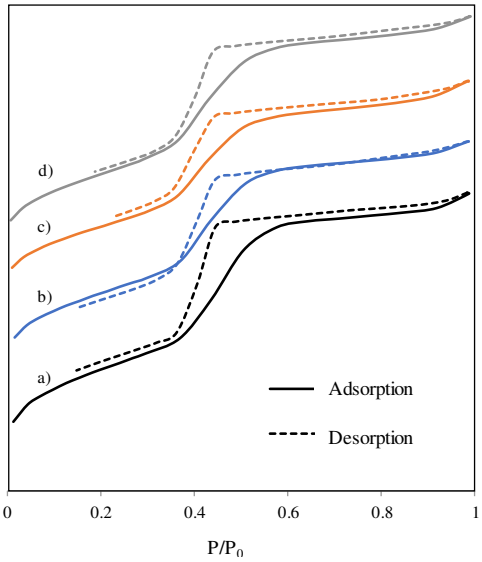

Figure 2. N_2 adsorption–desorption isotherms of a) parent MCM-41, b) Cu/MCM-41, c) Zr/MCM-41, and d) Cu/Zr/MCM-41.

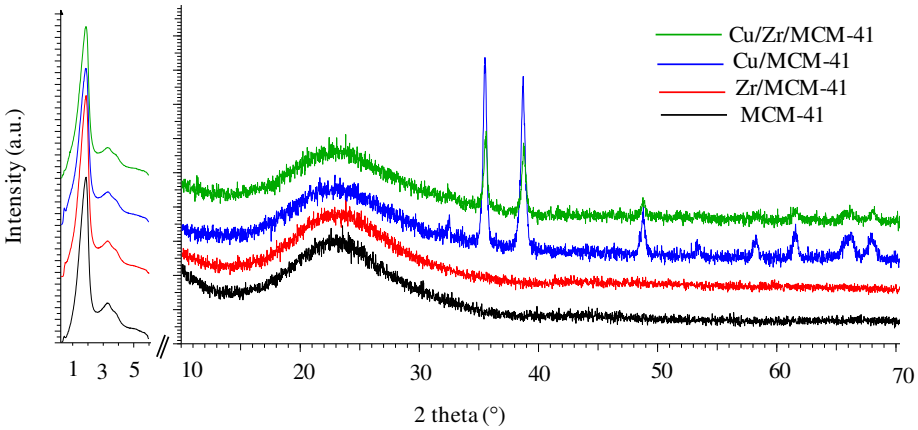

Figure 3. Low- and wide-angle XRD patterns of parent MCM-41, Cu/MCM-41, Zr/MCM-41, and Cu/Zr/MCM-41.

The low- and wide-angle XRD patterns (Figure 3) show the reflection peaks of the MCM-41 zeolite at 2θ=1.8°, 3.2°, and 5° before and after modification, corresponding to (100), (110), and (200) characteristic peaks of the amorphous mesoporous silica which suggesting that metal impregnation has insignificant effect on the structure of MCM-41 zeolite integrity [44, 46-50]. The wide-angle diffraction peaks at 2θ=35.5°, 38.6°, 48.8°, 53.3°, 58.1°, 61.5°, 65.6°, and 67.7° were attributed to Cu^{2+} form on Cu/MCM-41 and Cu/Zr/MCM-41 catalysts [34, 46, 51]. However, no specific peak representing Zr^{2+} (or any other forms of Zr) was observed over Zr/MCM-41, which may be attributed to the impregnation of Zr on the internal surface of MCM-41 zeolite.

The FT-IR spectra of the prepared catalysts, parent MCM-41, Cu/MCM-41, Zr/MCM-41 and Cu/Zr/MCM-41, are presented in the range of 400-4000 cm^{-1} in Figure 4. The results indicate that six bending vibration bands are observed for the zeolite catalysts prepared. There are hydroxyl groups on the surface as indicated with the broadband around 3440 cm^{-1} and the band around 1610 cm^{-1} are defined as the Si-OH deformational vibrations of adsorbed molecules [33, 34]. The internal and external asymmetric stretching of Si–O–Si groups are observed at around 805 cm^{-1} and 1090 cm^{-1} with a corresponding shoulder at 1239 cm^{-1} and the band at 465 cm^{-1} attributed to symmetric stretching modes of tetrahedral Si–O–Si and M–O–Si (M; metal) bending modes [31, 34, 35, 43, 49, 50]. As the adding metals on the zeolite, the absorption bands became stronger at 450-960 cm^{-1}, indicating the metals in the MCM-41 framework. Although parent MCM-41 material also exhibits these bands at the same range, the bands for parent MCM-41 are weak and the intensity of this band increases with metal incorporation in the framework [30, 37].

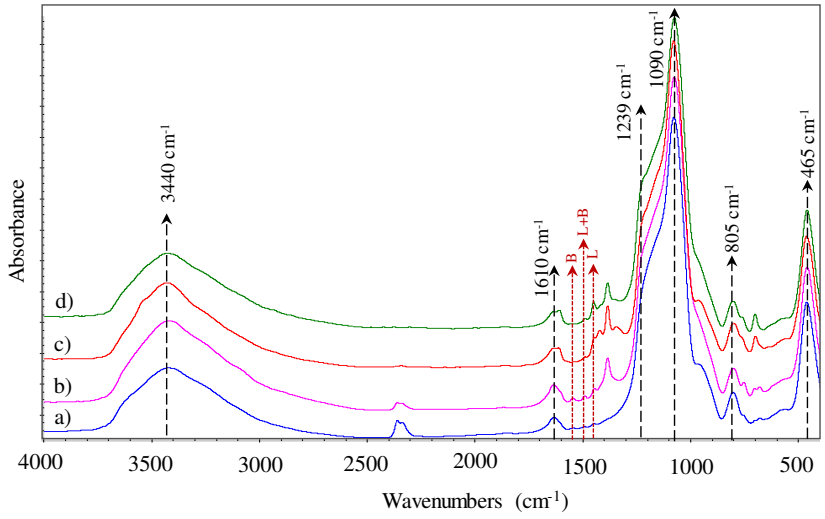

Figure 4. Py-IR spectrums of a) parent MCM-41, b) Zr/MCM-41, c) Cu/MCM-41, and d) Cu/Zr/MCM-41.

After the pyridine was impregnated on the catalyst, the acid sites of the catalysts presented between 1450-1550 cm^{-1} bands. The peak at around 1540 $cm^{-1}$was assigned to pyridine adsorbed on Bronsted (B) acid site. The interaction of pyridine molecule with Lewis (L) acid site give rise to a bending vibration at 1450 cm^{-1} and the band at 1500 cm^{-1} was attributed to both Brønsted and Lewis acid sites [37, 44]. Generally, Lewis acid sites define as weak acid sites [37]. The Lewis acid and Brønsted acid sites were not detected on the pure MCM-41. The amount of Brønsted and Lewis acid sites were obviously increased by the metals loading. After the Cu metal is impregnated, Lewis acidity peaks increase (as seen in Figure 4 (c)) and give the Cu/MCM-41 catalyst a weak acidity property. Zr impregnated MCM-41 shows strong Bronsted+ Lewis peak due to strong Bronsted acidity.

Table 2 shows the XRF measurements of the prepared zeolite catalysts. The Al in the framework of MCM-41 was replaced by impregnated metals, which increased the Si/Al molar ratio. This increase may be attributed to the dealumination, which occurs simultaneously with desilication, so Cu and Zr have mostly substituted Al. The mass ratio of impregnated metals was found about 10 % for Cu and Zr and 5-5% for Cu/Zr impregnation. Figure 5 illustrates the EDX mapping of MCM-41, Cu/MCM-41, Zr/MCM-41, and Cu/Zr/MCM-41 where

both Cu and Zr were successfully and homogenously impregnated over MCM-41 zeolite. Additionally, the impregnation of metal and bimetals have an insignificant effect on the morphology of MCM-41.

Table 2. XRF results of parent and metal impregnated MCM-41 zeolites.

Catalyst*	Al (wt%)	Si (wt%)	Cu (wt%)	Zr (wt%)	Si/Al
MCM-41	5.01	40.27	-	-	5.9
Cu/MCM-41	1.50	32.46	9.8	-	20.7
Zr/MCM-41	1.65	32.57	-	9.0	18.9
Cu/Zr/MCM-41	1.64	35.64	4.9	4.6	20.8

* MCM-41 represents the mixture of MCM-41/γ-Al_2O_3 having a ratio of 5:1.

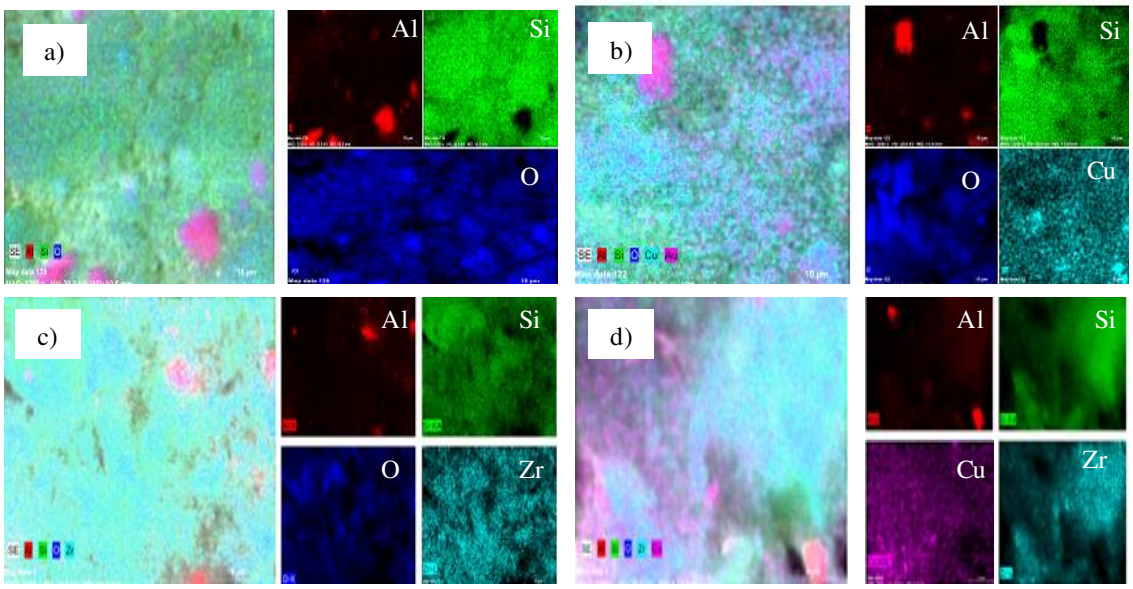

Figure 5. EDX mapping of a) MCM-41, b) Cu/MCM-41, c) Zr/MCM-41, and d) Cu/Zr/MCM-41.

3.2. Methylation of 2-methylnaphthalene

The methylation activity of mesoporous MCM-41 was enhanced by the impregnation of Cu, Zr, and Cu/Zr at lower WHSV conditions as shown in Figure 6. When WHSV was kept at 1 h^{-1}, the conversion of 2-MN increased from about 17 wt.% to approximately 35 wt.%, 30 wt.% and 22 wt.% with the impregnation of Cu, Zr, and Cu/Zr, respectively.

However, the conversion of 2-MN decreased with an increase in the WHSV as the residence time of reactants in the catalyst bed decreased with increasing WHSV. Additionally, at the highest WHSV (3 h^{-1}), the conversion decreased with the impregnation of Zr and Cu/Zr, which may be attributed to the narrowing of pore size, where the reactants can not reach the active sites efficiently. On the other hand, the pore dimension has demonstrated an expansion after the Cu impregnation which may explain the better conversion on the Cu/MCM-41 mesoporous. Consequently, the improvement in the catalytic performance on methylation reaction of 2-MN was mainly attributed to both the weakening of acid strength and the expansion of pore dimension that occurred after Cu incorporation into mesopore framework instead of Al. Similarly, Jin et al. [52] proved that the increase in conversion is convenient with the weakening of acid strength. Additionally, Güleç et al [8, 53] presented that the impregnation of Cu and Zr over MCM-41 zeolite was considerably enhanced the conversion in the

disproportionation of 2-MN. Furthermore, Morin et al. [54] suggested that the particular selectivity of MCM41 samples was most likely due to the presence of regular non-interconnected long channels, where the molecules undergo successive reactions of disproportionation and transalkylation before desorption.

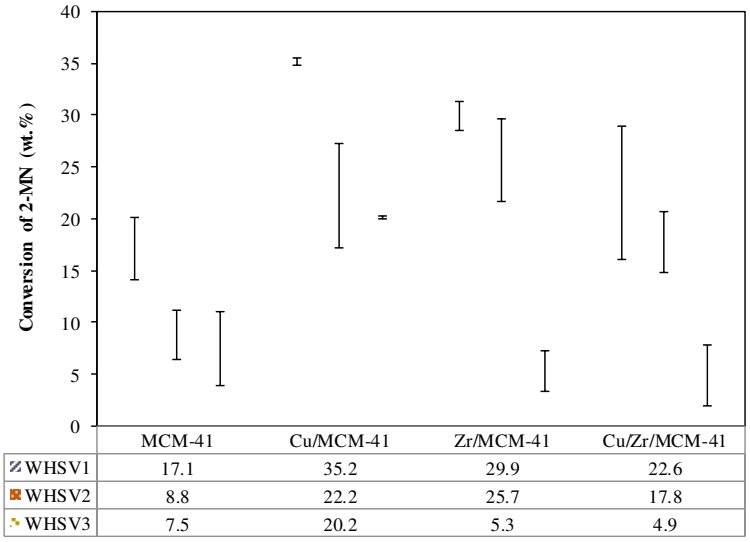

	MCM-41	Cu/MCM-41	Zr/MCM-41	Cu/Zr/MCM-41
WHSV1	17.1	35.2	29.9	22.6
WHSV2	8.8	22.2	25.7	17.8
WHSV3	7.5	20.2	5.3	4.9

Figure 6. Conversion of 2-MN over MCM-41, Cu/MCM-41, Zr/MCM-41, Cu/Zr/MCM-41 at 400 °C for different WHSVs.

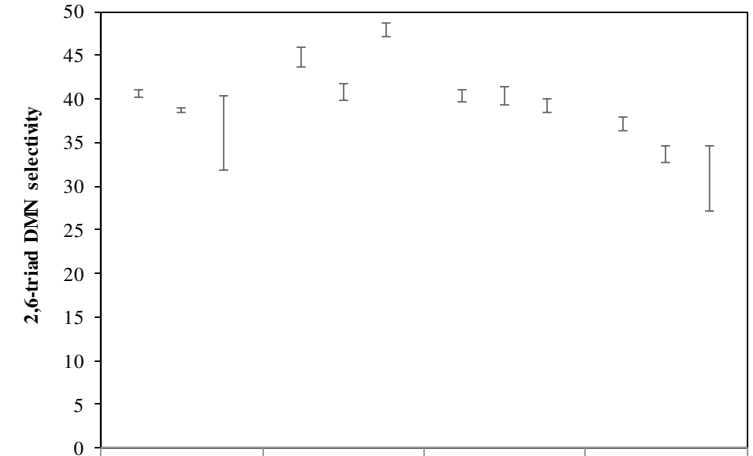

	MCM-41	Cu/MCM-41	Zr/MCM-41	Cu/Zr/MCM-41
WHSV1	40.6	44.8	40.3	37.2
WHSV2	38.7	40.8	40.4	33.7
WHSV3	36.1	47.9	39.3	30.9

Figure 7. Selectivity of 2,6-triad DMN over MCM-41, Cu/MCM-41, Zr/MCM-41, Cu/Zr/MCM-41 at 400 °C for different WHSVs.

The selectivity of 2,6-triad DMN over MCM-41, Cu/MCM-41, Zr/MCM-41, Cu/Zr/MCM-41, are presented in Figure 7. The selectivity was found approximately 40 wt.% for MCM-41, Zr/MCM-41, and Cu/Zr/MCM-41. It was slightly enhanced to about 48 wt.% over Cu/MCM-41, which was attributed to the weakening of acid strength and enlargement of pore dimensions, similarly [4, 52]. As the weak acid density may lead to slow deactivation of the catalyst, increased mesoporosity which is susceptible to methylation reaction. The

enlargement of the pore size may result in a reduction of unit cell dimensions, which can lead to the contraction of pore dimensions. The increase in mesopore volume was found to be parallel to the increase in selectivity to 2.6-triad DMN by decreasing the volume of unit cells [3, 4]. More reactants can therefore easily diffuse in and out of pore channels, which may help to increase 2,6-triad DMN selectivity [3].

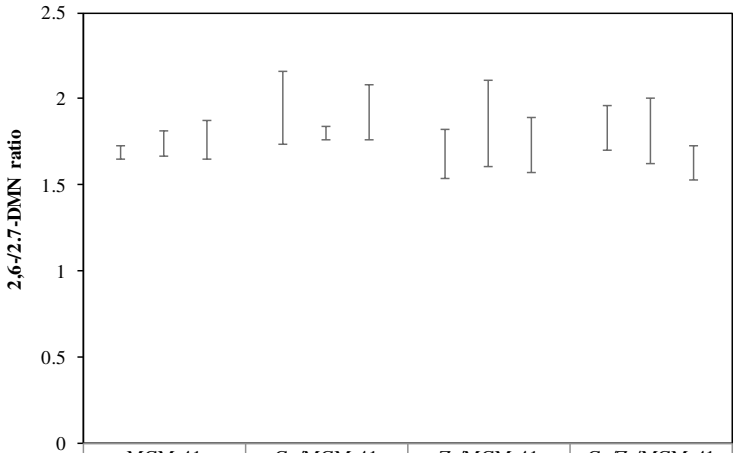

	MCM-41	Cu/MCM-41	Zr/MCM-41	Cu/Zr/MCM-41
WHSV1	1.69	1.95	1.68	1.83
WHSV2	1.74	1.8	1.86	1.81
WHSV3	1.76	1.92	1.73	1.63

Figure 8. Ratio of 2,6-/2,7-DMN over MCM-41, Cu/MCM-41, Zr/MCM-41, Cu/Zr/MCM-41 at 400 °C for different WHSVs.

As it is known that the higher ratio of 2,6-/2,7-DMN can enable an easy subsequent separation because a eutectic mixture would be formed at a ratio of 0.7 [11]. However, the dimension of 2,6-DMN is somewhat larger than that of 2,7-DMN, with their molecular dimensions in length, thickness and cylindrical diameter being 10.06 Å, 2.76 Å, 6.44 Å for 2,6-DMN and 9.73 Å, 2.76 Å, 6.03 Å for 2,7-DMN [52]. Therefore 2,7-DMN has less diffusion problem than 2,6-DMN once the products diffusing out from the pore channel of catalyst. The suitable pore structure is, therefore, highly important for higher 2,6-DMN/2,7-DMN ratio. Figure 8 shows that the 2,6-/2,7-DMN ratio was higher than 1.7 for all the catalysts tested in this study. The highest ratio was found as 1.95 for Cu/MCM-41, and Zr/MCM-41 and Cu/Zr/MCM-41 follows as 1.86 and 1.83, respectively. Jin et al. [52] mentioned that after the impregnation of Zr on ZSM-5, the unit cell volume has an expansion of 33.39 Å, which can reduce the negative ‘‘product selectivity’’ between 2,6-DMN and 2,7-DMN. Similarly, in this study, after Cu impregnation on MCM-41, the pore diameter of the catalyst decrease from 37.21 Å to about 31.03 Å while the pore volume increase from 0.71 to 0.80 cm^3/g. Therefore the increase in the 2,6-/2,7-DMN ratio may directly be attributed to the pore structure of MCM-41 after Cu impregnation.

3.3. Product distributions

Naphthalene based product distributions obtained from the methylation of 2-MN over parent MCM-41, Cu/MCM-41, Zr/MCM-41 and Cu/Zr/MCM-41, are presented in Table 3. The DMN distribution was found as 14.4 wt.% as the highest value once the methylation of 2-MN carried out over Cu/MCM-41, whereas it is only

about 3 wt.% for MCM-41, 7.7 wt.% for Zr/MCM-41 and 1.5% for Cu/Zr/MCM-41. Furthermore, nearly half of the DMN isomers are consisting of 2,6-triad DMN (2.6-DMN, 1,5-DMN and 1,6-DMN) for Cu/MCM-41.

Another critical issue is the isomerisation of 2-MN over the catalysts. However, the isomerisation level was kept minimal thanks to the large pores in the catalyst where the 2-MN molecules diffuse in the pore structure and give a methylation reaction over the active surface and both DMN isomers and unreacted 2-MN can easily be diffuse outside without further isomerisation of 2-MN to 1-MN. Therefore, the formation of 1-MN was kept minimal over MCM-41 type zeolite catalysts. Similarly, due to the pore structure, DMN isomers diffuse outside without further methylation reaction to TMN isomers. Thus, the formation of TMN isomers was also kept minimal.

Table 3. Product distributions of methylation of 2-MN over parent and metal impregnated MCM-41 zeolite catalysts for WHSV1.

Catalysts*	**MCM-41**	**Cu/MCM-41**	**Zr/MCM-41**	**Cu/Zr/MCM-41**
Naphthalene	**5.1 ± 1.5**	**16.4 ± 0.9**	**11.2 ± 0.3**	**1.6 ± 0.1**
Methylnaphthalenes	**85.6 ± 2.3**	**55.6 ± 1.5**	**73.0 ± 0.7**	**90.5 ± 0.6**
1-MN	1.9 ± 0.1	2.8 ± 0.1	2.2 ± 0.1	1.9 ± 0.1
2-MN	98.1 ± 0.1	97.2 ± 0.1	97.8 ± 0.1	98.1 ± 0.1
Dimethylnaphthalenes	**3.0± 0.9**	**14.4 ± 0.5**	**7.7 ± 0.1**	**1.5 ± 0.5**
2.6-DMN	15.7 ± 0.2	18.6 ± 0.3	16.9 ± 0.7	16.3 ± 0.2
2.7-DMN	8.5 ± 0.8	9.6 ± 0.9	10.5 ± 0.5	8.7 ± 0.6
1.3+1.7-DMN	40.2 ± 0.6	35.4 ± 0.7	38.4 ± 0.4	41.6 ± 1.5
1.4-DMN	8.5 ± 0.1	8.1 ± 0.1	9.1 ± 0.1	7.7 ± 0.2
1.6-DMN	21.6 ± 0.9	15.6 ± 0.3	19.7 ± 0.3	16.1 ± 0.3
1.5-DMN	3.3 ± 1.0	10.6 ± 1.2	3.4 ± 0.2	4.7 ± 0.4
1.2-DMN	1.0 ± 0.3	0.5 ± 0.0	0.9 ± 0.3	2.1 ± 0.8
2.3-DMN	0.2 ± 0.1	0.9 ±0.2	0.4 ± 0.1	0.4 ± 0.1
1.8-DMN	0.1 ± 0.1	0.4 ±0.0	0.5 ± 0.2	0.3 ± 0.1
Tri-methylnaphthalene	**0.4 ± 0.1**	**0.4 ± 0.3**	**1.1 ± 0.1**	**1.9 ± 0.1**

* MCM-41 represents the mixture of MCM-41/γ-Al_2O_3 having a ratio of 5:1.

4. Conclusions

The selective synthesis of 2,6-triad DMN from methylation of 2-MN was investigated over pure MCM-41, Cu/MCM-41, Zr/MCM-41, Zu/Zr/MCM-41, which has attracted considerable attention among M41S members due to its regular mesopores, large surface area, low acidity and good thermal stability. The conversion of 2-MN increased with the impregnation of Cu, Zr, Cu/Zr over MCM-41. The highest conversion of 2-MN was found as 35 wt.% over Cu/MCM-41 at WHSV1. Similarly, the highest 2,6-triad DMN selectivity (48 wt.%) and the highest 2,6-/2,7-DMN ratio (1.95) were also found over Cu/MCM-41. Furthermore, nearly half of the DMN isomers are consisting of 2,6-triad DMN (2.6-DMN, 1,5-DMN and 1,6-DMN) for Cu/MCM-41. The characterisation results demonstrated that the Cu is well connected on the MCM-41 framework to the enhanced pore structure of MCM-41 for selective synthesis of 2,6-triad DMN isomers. It is proposed as future work that the synthesis of Cu/MCM-41/Al_2O_3 by co-precipitation method would increase the catalyst performance in the methylation reaction. In order to reach higher conversion and selectivity values, optimum Cu ratio over MCM-41 zeolite catalyst would be tested.

Acknowledgement

This work was supported by The Scientific and Technological Research Council of Turkey [TÜBİTAK, Project No: 112M297].

References

[1] X. Wang, F. Guo, X. Wei, Z. Liu, Y. Wang, S. Guo, Russ. J. Phys. Chem. A, 93(3) 431-436 (2019).

[2] Y. Zhang, J. Feng, Z. Lyu, X. Li, Mod. Res. Catal. 3(02):19 (2014).

[3] J.-N. Park, J. Wang, S.-I. Hong, C.W. Lee, Appl. Catal. A, 292 68-75 (2005).

[4] L. Zhao, H. Wang, M. Liu, X. Guo, X. Wang, C. Song, H. Liu, Chem. Eng. Sci. 63(21) 5298-5303 (2008).

[5] Z. Liang, G. Xinwen, L. Min, W. Xiangsheng, S. Chunshan, Chin. J. Chem. Eng. 18(5) 742-749 (2010).

[6] L. Jin, X. Zhou, H. Hu, B. Ma, Catal. Commun. 10(3) 336-340 (2008).

[7] B. Viswanathan, B. Jacob, Catal Rev. 47(1) 1-82 (2005).

[8] F. Güleç, A. Niftaliyeva, A. Karaduman, Res. Chem. Intermed. 44(12) 7205-7218 (2018).

[9] A. Niftaliyeva, A. Karaduman, Anadolu Univ. J. Sci. Technol. A Appl. Sci. Eng. 16(2) 275-282 (2015).

[10] T. Chen, N. Kang, C. Lee, H. Kim, S. Hong, H. Roh, Catal. Today. 93 371-3766 (2004).

[11] R. Millini, F. Frigerio, G. Bellussi, G. Pazzuconi, C. Perego, P. Pollesel, U. Romano, J. Catal. 217(2) 298-309 (2003).

[12] S.-B. Pu, T. Inui, Appl. Catal. A 146(2) 305-316 (1996).

[13] M. Liu, W. Wu, O. Kikhtyanin, L. Xiao, A. Toktarev, G. Wang, Microporous and Mesoporous Mater. 181:132-140 (2013).

[14] F. Güleç, A. Özen, A. Niftaliyeva, A. Aydın, E.H. Şimşek, A. Karaduman, Res. Chem. Intermed. 44(1) 55-67 (2018).

[15] C. Zhang, X. Guo, C. Song, S. Zhao, X. Wang, Catal. Today 149(1) 196-201 (2010).

[16] G. Watanabe, Y. Nakasaka, T. Taniguchi, T. Yoshikawa, T. Tago, T. Masuda, Chem. Eng. J. 312 288-295 (2017).

[17] A. Niftaliyeva, F. Güleç, E.H. Şimşek, M. Güllü, A. Karaduman, Anadolu Univ. J. Sci. Technol. A Appl. Sci. Eng. 16(2) 167-178 (2015).

[18] K. Bobuatong, M. Probst, J. Limtrakul, J. Phys. Chem. C. 114(49) 21611-21617 (2010).

[19] C. Li, L. Li, W. Wu, D. Wang, A. Toktarev, O. Kikhtyanin, Procedia Engineering 18:200-205 (2011).

[20] T. Tsutsui, K. Ijichi, T. Inomata, T. Kojima, K. Sato, Chem Eng. Sci. 59(19) 3993-3999 (2004).

[21] C. Zhang, X.W. Guo, Y.N. Wang, X.S. Wang, C.S. Song, Chin. Chem. Lett. 18(10) 1281-1284 (2007).

[22] A. Chobsa-Ard, N. Kraikul, P. Rangsunvigit, S. Kulprathipanja, Chem. Eng. J. 139(1) 78-83 (2008).

[23] X. Wang, W. Zhang, L. Zhao, Iran J. Chem. Chem. Eng. 34(3) 19-24 (2005).

[24] Y. Fang, H. Hu, Catal. Commun. 7(5) 264-267 (2006).

[25] N. Kraikul, P. Rangsunvigit, S. Kulprathipanja, Chem. Eng. J. 114(1-3) 73-79 (2005).

[26] N. Kraikul, P. Rangsunvigit, S. Kulprathipanja, Adsorption 12(5-6) 317-327 (2006).

[27] N. Kraikul, P. Rangsunvigit, S. Kulprathipanja, Chem. Eng. J. 131(1-3) 145-153 (2007).

[28] K. Lin, PP. Pescarmona, K. Houthoofd, D. Liang, G. Van Tendeloo, PA. Jacobs, J. Catal. 263(1) 75-82 (2009).

[29] R. Luque, JM. Campelo, D. Luna, JM Marinas, AA. Romero, J. Mol. Catal. A. Chem. 269(1-2) 190-196 (2007).

[30] SK. Roy, D. Dutta, AK. Talukdar, Mater. Res. Bull. 103:38-46 (2018)

[31] X. Zhang, J. Dong, Z. Hao, W. Cai, F. Wang, Transactions of Tianjin University 24(4) 361-369 (2018)

[32] S. Haemi-myun, Int. J. BioSci. BioTech. 8(3) 171-182 (2016).

[33] K. Guo, F. Han, Z. Arslan, J. McComb, X. Mao, R. Zhang. Water, Air, & Soil Pollution 226(9) 288 (2015).

[34] C. Huo, J. Ouyang, H. Yang. Sci Report 4:3682 (2014).

[35] K. Murthy, S. Kulkarni, M. Chandrakala, KK. Mohan, P. Pal, TP. Rao, J. Porous Mater 17(2) 185-196 (2010).

[36] S. Udayakumar, A. Pandurangan, P. Sinha. Appl. Catal. A. 272(1-2) 267-279 (2004).

[37] B. Xue, J. Xu, P. Liu, L. Lv, C. Xu, Y. Li, J. Mol. Catal. A: Chem. 357:50-58 (2012).

[38] KG. Bhattacharyya, AK. Talukdar, P. Das, S. Sivasanker. J. Mol. Catal. A: Chem. 197(1-2) 255-262 (2003).

[39] C. García-Sancho, R. Moreno-Tost, J. Mérida-Robles, J. Santamaría-González, A. Jiménez-López, P. Maireles-Torres. Appl. Catal. A. 433:179-187 (2012).

[40] J. Ding, T. Ma, M. Cui, R. Shao, R. Guan, P. Wang, Molecular Catalysis 461:1-9 (2018).

[41] F. Güleç, F. Sher, A. Karaduman. Petroleum Science 16(1) 161-172 (2019).

[42] R. Juarez, A. Padilla, A. Corma, H. Garcia. Catal. Commun. 10(5) 472-476 (2009).

[43] MSA. Salam, MA. Betiha, SA. Shaban, AM. Elsabagh, RMA El-Aal. Egyptian Journal of Petroleum 24(1) 49-57 (2015).

[44] DP. Gamliel, BP. Baillie, E. Augustine, J. Hall, GM. Bollas, JA. Valla. Microporous and Mesoporous Mater 261 18-28 (2018).

[45] LP. Ozorio, R. Pianzolli, L. da Cruz Machado, JL. Miranda, CC. Turci, AC. Guerra, Appl. Catal. A. 504 187-191 (2015).

[46] H. Kim, E. Jang, Y. Jeong, J. Kim, CY. Kang, CH. Kim, Catal. Today 314:78-93 (2018).

[47] I. Graça, M. Bacariza, A. Fernandes, D. Chadwick. App. Catal. B. Env. 224 660-670 (2018).

[48] C. López-Aguado, M. Paniagua, J. Iglesias, G. Morales, JL. García-Fierro, JA. Melero, Catal. Today 304 80-88 (2018).

[49] X. Dai, F. Qiu, X. Zhou, Y. Long, W. Li, Y. Tu, Electrochimica Acta 144 161-167 (2014).

[50] R. Tayebee, M. Amini, M. Akbari, A. Aliakbari. Dalton Transactions 44(20) 9596-9609 (2015).

[51] X. Wang, Y. Zhang, P. Ning, S. Yan, L. Wang, Q. Ma, RSC Advances 7(89) 56638-56647 (2017).

[52] L. Jin, Y. Fang, H. Hu. Catal. Commun. 7(5) 255-259 (2006)

[53] F. Güleç, E.H. Simsek, A. Karaduman, J. Fac. Eng. Archit. Gazi Univ. 31(3) 610-621 (2016).

[54] S. Morin, P. Ayrault, S. El-Mouahid, N. Gnep, M. Guisnet, App. Catal. A 159(1-2) 317-331 (1997).